On estimating the probability to reach $Q = P_{fus}/P_{aux}$ larger than a specified lower bound in ITER.

by

Otto J.W.F. Kardaun

Abstract A simplified analysis is given of the problem to estimate the 'probability' for ITER to attain a power amplification factor Q of at least 10. Attention is almost entirely restricted to the parameters of ITER FEAT. The connotational framework of the word 'probability' is briefly discussed and the propagation of uncertainty following from the interval estimate of the confinement time is derived (a) for ITER operation at constant fusion output power, and (b) for operation at a temperature that maximises $Q = P_{fus}/P_{aux}$. The second situation requires a radial integration of the local power balance. Instead of a local transport model, a simple class of temperature profiles is used. The results are represented graphically. A generalisation of the widely used fusion triple-product plot against temperature is suggested. The analysis presupposes that at the reference operating point in situation (a), and in the range of operating temperatures projected in situation (b), the conditions to reach standard ELMy H-mode in ITER are met.

— *1. Introduction* —

The international ITER project is being actively pursued [1], while serving both as a blueprint for an international Next Step tokamak experiment and as a focussing element for present-day tokamak investigations.

In [2, 3] a practical statistical approach has been developed for interval estimation of the global energy confinement time of a plasma in ITER FDR [2], based on the empirical evidence from a multi-machine H-mode database [2, 4].

Such type of estimates are made under the presupposition that the reference operating point in ITER respects the operational boundaries for reaching (ELMy) H-mode, such as the Troyon beta limit, the Greenwald density limit, the power threshold limit and possibly a radiation limit, see [3, 5, 6].

Recently, the problem has been raised [7] to generalise this result by assessing the probability that ITER will achieve an amplification factor $Q = P_{fus}/P_{aux}$ between fusion power and auxiliary heating power of at least a specified lower bound (say, 50 for ITER FDR, 10 for the reduced-cost ITER FEAT). In fact, in a somewhat more general context, the question was asked [7] to estimate the probability that ITER will achieve its main scientific (e.g. $Q > 10$) and technological (e.g. a wall fluence of at least 0.3 MW$a/m^2$) objectives. Here we simplify the problem by restricting attention to the uncertainty in $Q = P_{fus}/P_{aux}$ due to the uncertainty in the confinement time prediction. The latter one is based on arguments, derived in [3], that are complementary to those described in the pioneering paper [8]. While considering the operating temperature as an explicit parameter throughout, this paper provides some background to more extensive ITER FEAT calculations described in [13]. We start with a description of the probabilistic context.

— *2. Probability interpretation* —

First let us reflect a little about the meaning of the word probability in this context. In classical

IPP Garching 2000, Max-Planck-Institut für Plasmaphysik, Boltzmannstraße 2, D-85748 Garching.

statistics a probability is interpreted as the limit of a relative frequency for a certain type of event to happen in a series of (nearly) identical experiments. In that case, an empirical justification exists for a number of basic relationships between probability statements, as expressed in the Kolmogorov axioms, and for their mathematical consequences, such as Bayes' theorem. In the context of ITER confinement time prediction, several 'definitions' have been given of the concept of a confidence interval. These led to the notion of a single, practical interval estimate, which can be viewed as the specification of some quantiles of a credence distribution (in the sense of distributional inference [9] of the confinement time. (The word credence is used to distinguish it from a frequency-based probability.) In a Bayesian approach, 'probability' is used as a quantitative expression for the personal strength of conviction, elicited e.g. by betting behaviour, a person (purports to) attach to a proposition. One feature of this approach is that the extensional context of the word 'probability' is much larger than that for the classical frequency-based definition of probability, so that sentences like "the 'probability' of ITER (as a unique experiment) to reach its stated aims", are covered by it. Another feature of this approach, however, is that the algorithmic rules derived from Kolmogorov's axioms do not have an empirical basis for this enlarged context, and in fact do not need to hold, unless one is a follower of the Bayesian school of statistics and stipulates *ab initio* that any "rational" person should employ such rules when reasoning with 'probabilities'. Bayesians tend to gloss over the fact that serious semantic difficulties can arise when (conditional) probabilities are used in a non frequency-based situation. We mention that other mathematical rules for reasoning with degrees of personal conviction have been advocated e.g. by [10] and [11] and are now incorporated in fuzzy set theory, see eg. [12]. In this text, for clarity, we shall reserve the word probability (without using quotes) for the frequency-based definition, and use, somewhat interchangeably, the words 'probability', credence for the non-frequency based (Bayesian as well as distributional-inference based) definitions in case of a unique event.

For concreteness we briefly state here some of the rules following from the Kolmogorov axioms, available of course in almost any textbook on probability theory. If A_1 and A_2 are 'events', or 'outcomes' of a random experiment, with probability $P(A_1)$ and $P(A_2)$, respectively (both unequal to zero), then

$$P(A_1 \cap A_2) = P(A_1)P(A_2|A_1) = P(A_2)P(A_1|A_2) \tag{1}$$

and

$$P(A_1 \cup A_2) = P(A_1) + P(A_2) - P(A_1 \cap A_2). \tag{2}$$

(Extensions exist for more than two events.) The intersection symbol $(A_1 \cap A_2)$ is used to denote the event that both event A_1 and event A_2 occur; $P(A_2|A_1)$ means the probability that A_2 occurs, given that A_1 occurs. By definition, if A_1 and A_2 are independent events, then $P(A_2|A_1) = P(A_2)$ and hence $P(A_1 \cap A_2) = P(A_1)P(A_2)$. Also of interest is the marginalisation rule, which states that

$$P(A) = \sum_{i=1}^{n} P(A|A_i) \tag{3}$$

if $A_1, \ldots, A_n$ are mutually exclusive $(A_i \cap A_j \neq 0)$ and exhaustive $(\bigcup_{i=1}^{n} A_i = \Omega$, the entire outcome space with $P(\Omega) = 1)$. In a plasma physical context, the marginalisation rule implies for instance

$$P\{Q > 10\} = \int P\{Q > 10|P_{aux} = p\} f_{P_{aux}}(p)dp \tag{4}$$

where $f_{P_{aux}}(p)dp = P\{p < P_{aux} < p + dp\}$. Here, we follow the Bayesian paradigm for a moment while glossing over the precise meaning of such an unconditional 'probability': removing a condition by marginalisation yields 'probabilities' that are a (weighted) average, not e.g. the maximum (or 'envelope') of the conditional 'probabilities'.

Let us first make some general remarks on assessing $P\{Q > 10\}$, and make a concrete evaluation in a very simplified context later. The attributed credence should satisfy

$$P\{Q > 10\} = P\{Q > 10|Tech\ Spec\}P\{Tech\ Spec\} \tag{5}$$

where $Tech\ Spec$ stands for the condition that the technical specifications of the machine are realised 'within time and budget'. Evidently, with additional time and budget for the critical path activities ('contingency reserve'), obstacles to achieve the technical specifications can be worked around, thus increasing $P\{Q > 10\}$. Actually, it is very diffult to estimate $P\{Q > 10\}$. In fact, assignment of such a 'probability', except perhaps in a subjective manner, seems to be rather far remote from the actual working practice to achieve such type of technical aims when reconstructing present-day machines.

In principle, one could imagine to break down the route to reach a specified technical goal into a network of activities, some of them in series (i.e. necessary sequential steps), and others in parallel (i.e. alternative solutions or fall-back options). Corresponding to this network, one can decompose the desired unconditional probability into sums and products of conditional 'probabilities', according to the two probability rules, stated above, that follow from the Kolmogorov axioms. These conditional 'probabilities' are then to be assessed and regularly updated. The set-up of such a system might have as 'spin-off value' that it invites to proceed along a more or less systematic way to monitor progress even if the conditional 'probabilities', starting with mere guesses, are given the (weak) empirical status they ontologically deserve. Obviously, surges of enthusiasm and dedication, scientific-technological breakthroughs and other 'unexpected events' are not incorporated in such an approach.

Here we simplify the problem drastically by assuming that the technical requirements (as specified e.g. in the ITER Physics Basis Document [2] are realised. Hence, $P\{Q > 10|TechSpec =' OK'\}$ depends on (a) the uncertainty in the prediction of the actual global confinement time in ITER, (b) the uncertainty in the operational boundaries to reach H-mode, (c) the uncertainty in the 'natural' or 'shaped' profiles of n_e, T_e and current density, in the impurity and He ash concentration, etc. In this note, we simplify further by neglecting both aspects (b) and (c). In practice, undeterminable uncertainties are replaced by assumptions, that are, hopefully, slightly conservative, e.g. by staying some 20% below the Greenwald limit, and, say, some 40% above the power threshold as well as below the (ideal) beta limit. The confinement reduction from resistive MHD modes, just below the ideal beta limit, tends to occur in the upper region of the estimated confinement time interval, see Fig. 1 in [2] and Figs. 1 and 2 in [14]. Therefore, such a reduction does seem of primary concern for ITER only if these modes occur at much lower beta values in ITER than in present-day machines, in which case one has to resort to active methods of stabilisation [15].

In the view of the author, the uncertainties in the operational limits are considerable, and a certain, albeit fairly limited, value consists in trying to express these uncertainties in a probabilistic way, since the real corrections are to be sought in an improved functional dependence (and specification of the influence of hidden variables). To some extent, this applies also for the confinement time. In that sense the interval estimate [2, 3] has to be considered as a *locum tenens* for such physical improvements.

— *3. Uncertainty propagation at constant P_{fus}* —

For illustrative purposes, we will consider now the propagation of (1) the inaccuracy $\Delta\tau_E$ in the confinement time and (2) the inaccuracy $\Delta\alpha_P$ in the exponent of the power dependence of the confinement time in ITER into an inaccuracy ΔQ in the power multiplication factor. We distinguish between two cases: (a) operating at constant P_{fus} (and hence constant T), which

will be discussed in the next section, and (b) varying (through P_{aux} and P_{rad}) the operating temperature T so as to maximise Q, to be discussed in this section.

We start with the (simplified) 0-D power balance at the separatrix:

$$0.2\eta_\alpha p_{fus}(n_D,T) - p_{rad,\mathrm{ff}}(Z_{\mathrm{eff}},n_e,T) - \eta_{rad,sep}p_{rad,xb} + p_{aux} = P_L/V = 3n_eT/\tau_E + 3d/dt(n_eT) \quad (6)$$

where $p_{rad,\mathrm{ff}}$ stands for the average loss power per volume due to Bremsstrahlung and cyclotron radiation (by free electrons), and $p_{rad,xb}$ for the loss power per volume due to recombination radiation ('fb') and line radiation ('bb'). The latter is considered as a control variable, together with p_{aux}. The quantity η_α is the heating efficiency of the alpha particles. For definiteness, we assume here, in basic agreement with [32], $Z_{\mathrm{eff}} \simeq 1.8$, $n_H/n_e = 0.01$, $n_{Be}/n_e = 0.02$, $n_C/n_e = 0.005$, $n_O/n_e = 0.005$, n_{He}/n_e determined by $\tau^*_{He}/\tau_{E,th} = 5$, $n_D/n_e = n_T/n_e$ determined by charge neutrality, $T_e = T_i = T$, $\eta_\alpha = 0.95$, $P_{ohm} = 1$ MW, and $P_{rad,xb} = 20$ MW, of which a fraction $\eta_{rad,sep} = 1/3$ is radiated inside the separatrix. We neglect beam-power losses from charge exchange, unconfined orbits and magnetic ripple effects, as well as possible 'transition radiation' effects [33]. We also neglect here the plasma rotation and the fusion contribution from the fast beam particles. We consider the ratio between line average, volume average and central values of n_e and T be subsumed in form factors, see [17]. For practical evaluation we use a flat n_e profile, which is considered to be realistic for standard ELMy H-mode operation (see [2], Ch.1, Fig.2 and [5], Fig. 1) and leads to lower Q values than do peaked density profiles achievable in strong ('box') and weak ('parabolic') Internal Transport Barrier modes [36, 37] as well as in pellet refuelled discharges [38]. Furthermore, we use a simple class of T profiles, as specified below. The main emphasis is on the functional dependence of the various terms in the power balance on the temperature.

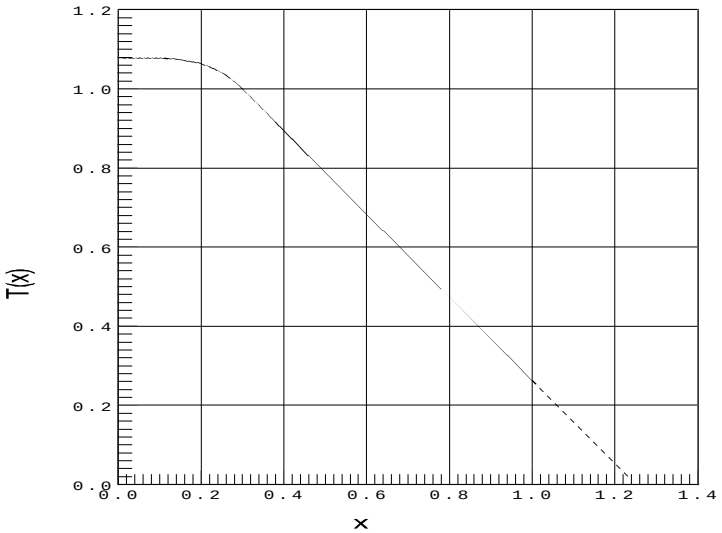

Figure 1: *A canonical (sawtooth averaged) temperature profile used to obtain integrated values P_{fus}, P_{rad}, and $< T >$ in the power balance equation. Model profiles of this shape are used for the numerical results displayed in the subsequent figures. In the plot, the value of T_c at $x = c = 0.3$ has been normalised to 1. For $x < 0.3$ temperature flattening due to sawteeth is expected. The results do not depend strongly on the profile shape in the outer region of the plasma.*

Using values from [18], we approximate the temperature dependence of the DT reactivity $< \sigma v > [m^3/s]$ for T between 3 and 30 keV by $10^{-26.2}T^{6.1-1.8\log(T)}$. This expression is accurate within some 1%. (Near T = 10 keV it yields $10^{-20.1}T^{2.5}$.) Hence, using 3.5 MeV energy per α

particle, we write

$$p_{fus} = 4.2 F_{fus} n_{e,20}^2 T^{6.1-1.8\log(T)} \quad [W/m^3, keV] \tag{7}$$

where F_{fus} is a form factor, obtained by integrating over the profiles. For the power loss from Bremstrahlung and cyclotron radiation (high-temperature cylindrical Trubnikov approximation with some 50% accuracy [22, 23]) we use, according to [19, 23, 21, 20], and inserting for ITER FEAT the parameters $B_t = 5.3T$, $a = 2m$, $R = 6.2m$:

$$\begin{aligned} p_{rad,ff} = & \\ & 4.8 \cdot 10^3 F_{br} Z_{\text{eff}} n_{e,20}^2 T^{0.5} \\ & + 19.2 F_{cy} F_{RH} T^{2.5} n_{e,20}^{0.5} a^{-0.5} (1 + 5.8 T^{-0.5})^{1/2} \quad [W/m^3, keV] \end{aligned}$$

where $F_{RH} = (f_H + (1 - f_H)(1 - R_{\text{eff}})^{0.5})$ with f_H the hole fraction, and R_{eff} the effective wall reflection coefficient, which we assume to be 0.15 and 0.85, respectively. The second factor in the cyclotron radiation term accounts for the toroidal magnetic field variation ($B \sim 1/R$) [23]. The form factors are obtained by integrating over the temperature profile and parametrised flux surface contour length (assuming toroidal symmetry) as described in section 4. For ITER FEAT parameters, the ratio between cyclotron radiation and Bremsstrahlung, according to the above formula and a temperature profile as in Fig. 1, varies between 2.5% at $< T >= 3$ keV and 15% for $< T >= 8$ keV.* Plasma diagnostics by ECE are well developed, see e.g. [24, 25, 26]. From a fundamental point of view, it is still worthwhile to accurately check the theoretical scalings of cyclotron emission and absorption against experiment, following pertinent investigations in this direction [27, 28, 29].

To determine the operating temperature (and hence the value of Q that will be achieved) a confinement time scaling is needed in Eq. (6). We use ITERH-98P(y,2) times a multiplication factor H_H. For ITER FEAT ($I_p = 15.0MA$, $Vol = 815m^3$, $k_a = Vol/2\pi^2 a^2 R = 1.7$, $M = 2.5$) this amounts to:

$$\tau_{E,th} = 3.28 H_H n_{e,20}^{\alpha_n} (P_L/100\text{MW})^{-\alpha_P} s. \tag{8}$$

with $\alpha_n = 0.41$ and $\alpha_P = +0.69$. First, we consider the error propagation of an uncertainty of $\pm 20\%$ (corresponding to one estimated technical standard error), in the point prediction of $\tau_{E,th}$, i.e., $\Delta ln(H_H) = 0.2$. The influence on $Q = p_{fus}/p_{aux}$ depends on what is kept constant. If P_{aux} is used to compensate for $\Delta ln(H_H)$ while keeping T (and hence p_{fus}) as well as n constant, one can directly derive the linear approximation

$$\Delta \ln(Q) = -\Delta \ln(p_{aux}) = (1 - \alpha_P)^{-1} \frac{p_L}{p_{aux}} \Delta ln(H_H) \tag{9}$$

Since the relation between H_H and Q is monotonic, a 'probability' statement for H_H directly transforms into a 'probability' statement for Q. [For instance, if the reference operating point would be chosen such that $Q = 10$ for $H_H = 0.8$, then, $P\{Q > 10\} = P\{H_H > 0.8\} \simeq 5/6$. For $P_L = 88$ MW, $P_{aux} = 40$ MW, a reference scenario in [32], and $\alpha_P = 2/3$, we would have

*The underlying theory is interesting but quite intricate [19, 21]. The cyclotron radiation in ITER FEAT is actually expected to be in a regime intermediate between 'tenuous' and 'high density' plasma as well and between 'low' and 'high temperature' plasma limit [21], which complicates analytic theoretical predictions. Ref. [34] contains a formula for the cyclotron radiation which takes the temperature profile effect and elongation somewhat differently into account, and agrees quantitatively within a factor of two with the cyclotron radiation power calculated from the (temperature-profile integrated) formula above, while giving only a slight modification of the ignition curves (Figs 2, 3 and 4). A more detailed comparison is especially important for advanced fuel ($D-^3He$) fusion reactor studies [35], where, due to the elevated temperature, synchrotron radiation plays a more substantial role in the power balance.

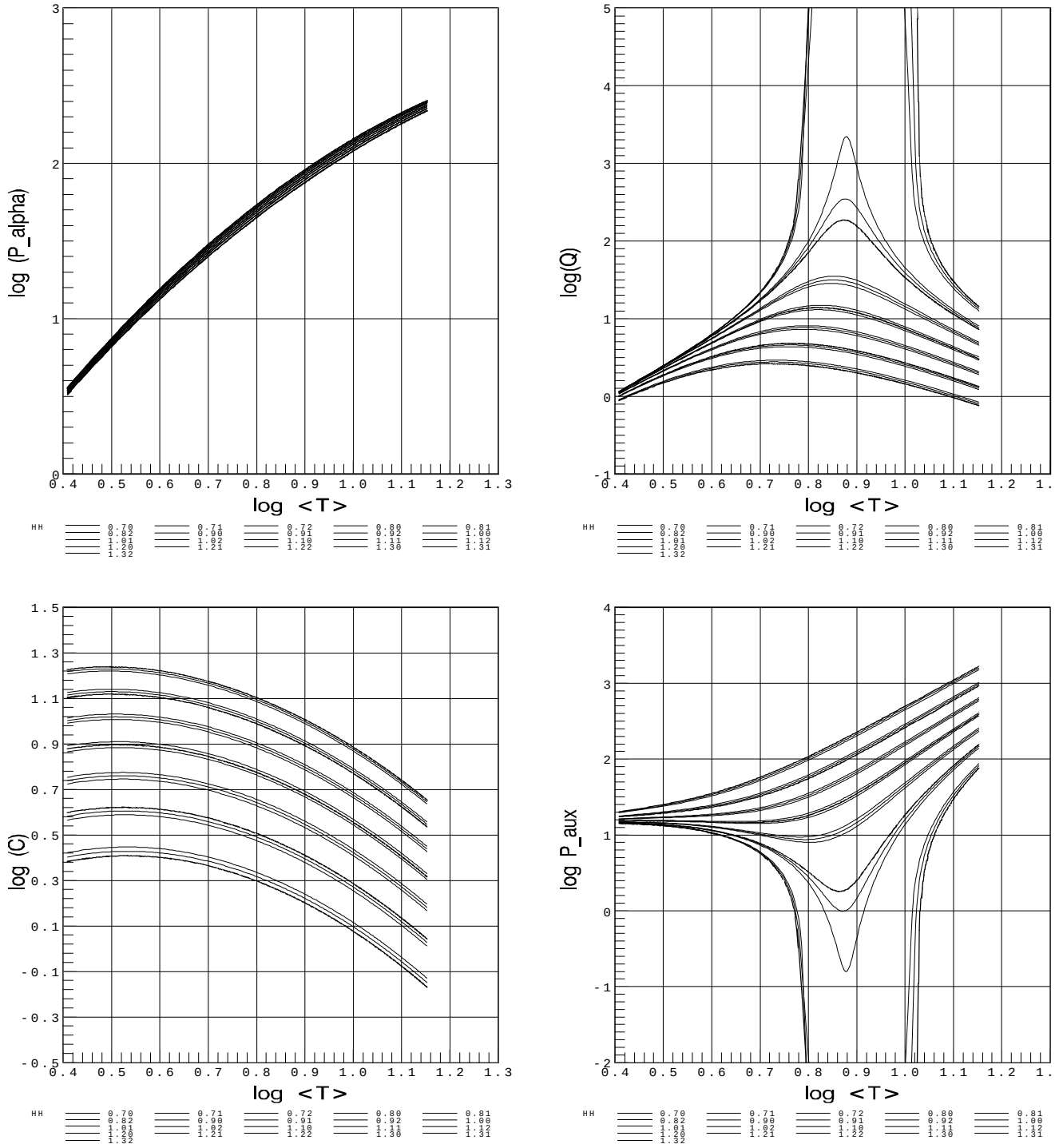

Figure 2: *Operating plots for ITER FEAT, as specified in the text, on a logarithmic scale. (a) The heating power from alpha particles as a function of the average temperature* $< T >$. *(b) The energy amplification factor* $Q = P_{fus}/P_{aux}$ *as a function of* $< T >$, *according to Eq. (6) while using the confinement time scaling* H_H *times ITERH-98P(y,2). The different curves correspond to* $H_H = 0.7$ *to 1.3 with minor steps of 0.01 and major steps of 0.1. (c) The ratio* $C = P_{fus}/P_L$ *as a function of* $< T >$ *for various values of* H_H. *(d) The auxiliary power* P_{aux} *needed to maintain an average operating temperature* $< T >$ *for various values of* H_H. *In the region where the slope is positive (negative) the operating point is thermally stable (unstable).*

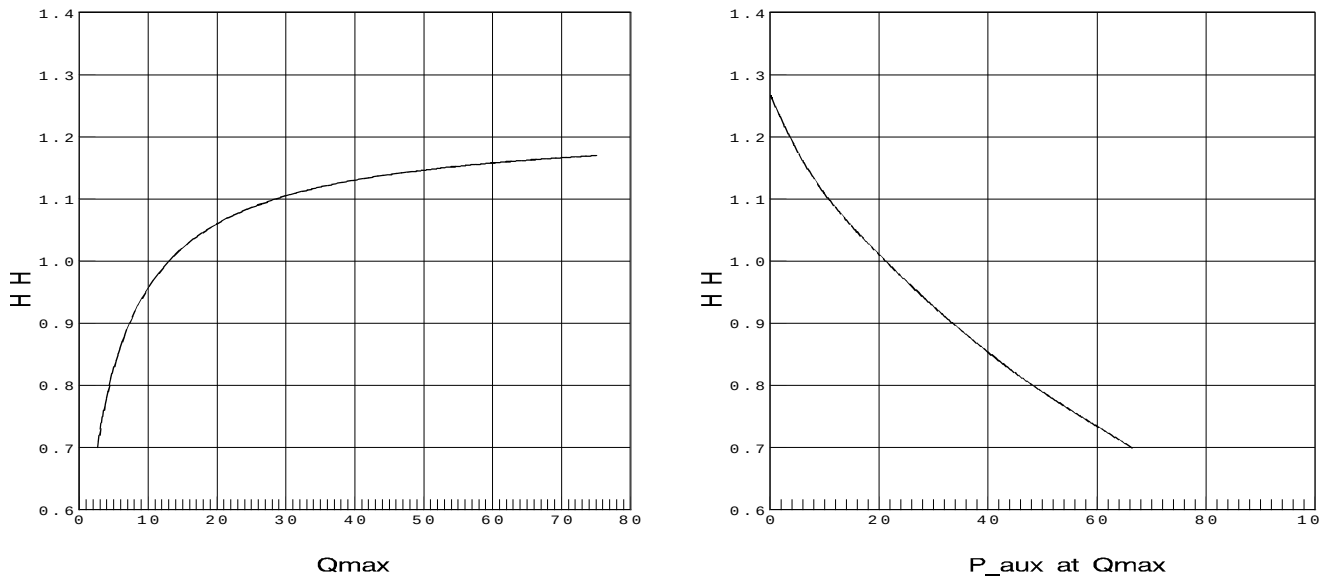

Figure 3: *(a) The horizontal axis describes the maximum value of* $Q = P_{fus}/P_{aux}$ *that can be obtained as a function of the confinement-time multiplication factor* H_H*. (b) The horizontal axis describes, as a function of* H_H*, the value of* P_{aux} *needed to attain an operating temperature* $< T >$ *that maximises the value of* $Q = P_{fus}/P_{aux}$*.*

$\Delta(\ln(Q)) = 6.6\Delta ln(H_H)$ and $P\{H_H < 1.2\} = P\{Q < 140\} \simeq 5/6$ at constant $P_{fus} = 400$MW.] One can immediately deduce that, if the reference operating point satisfies $Q = 10$ for $H_H = 1.0$, as actually in [32], then $P\{Q > 10\} = P\{H_H > 1.0\} \simeq 1/2$ and $P\{H_H > 0.8\} = P\{Q > 2.3\} \simeq 5/6$ for constant $P_{fus} = 400$MW. However, as we shall see in the next section, $\{Q > 10\}$ can be increased by lowering somewhat the operating temperature and hence the fusion output power P_{fus}. It is noted that above $Q \simeq 50$, compared to $Q \simeq 10$, the linear approximation between $\ln(Q)$ and $\ln(H_H)$ breaks down. At the same time, for practical purposes, a plasma with any $Q > 50$ can be considered to be in a state of 'essentially self-sustained burn' in the sense that P_{fus} is much larger than the auxiliary power P_{aux} needed for burn control.

The interval estimate for $\tau_{E,th}$ includes the propagation of the uncertainty in the regression exponents of the empirical scaling. However, just for curiosity we will digress for a moment while looking at the propagation of uncertainty from a single exponent. As an example, we take $\alpha_P \pm \Delta\alpha_P = 0.7 \pm 0.05$. For a simple power-law scaling, $\tau_E = H_H P_L^{\alpha_P}$, we have $\Delta \ln \tau_E = -\ln(P_L/P_{L,\mathrm{ref}})\Delta\alpha_P$, where $P_{L,\mathrm{ref}}$ is the reference power, defined as the power for which τ_E is the same for all α_P. Combining this expression with Eq. (9), we get

$$\Delta \ln(Q) = -(1-\alpha_P)^{-1} \frac{P_L}{P_{aux}} \ln(\frac{P_L}{P_{\mathrm{ref}}})\Delta\alpha_P \tag{10}$$

Choosing, rather arbitrarily, e.g. $P_{L,\mathrm{ref}} = 3MW$, a value close to the center of gravity of the ITERH.DB3 database, we get for example, with $P_L = 85MW$ and $P_{aux} = 40MW$, $\Delta \ln Q = 1.2$, i.e. $(\underline{Q}, \overline{Q}) = (3.0, 33)$. On the other hand, for $P_{L,\mathrm{ref}} = P_{L,ITER}$ we get $\Delta \ln(Q) = 0$. Obviously,

when the point prediction of $\tau_{E,th}$ of the scaling is correct at the ITER reference parameters, then the local power degradation of $\tau_{E,th}$ *around* the reference operating point is immaterial for the uncertainty in the prediction of $\tau_{E,th}$, and hence of Q, *at* the operating point. The ITER experiment itself will have to provide experimental information in how far for instance collective alpha particle instabilities, see [2] Ch. 5, influence the power dependence of the global energy confinement time around the reference operating point.

Presenting the 'probability' to reach $Q > 10$ at constant, specified P_{fus} has some distinctive feature in that the costs per 'virtual' kwh energy production are directly inversely proportional to P_{fus}. This 'economic' point of view, more appropriate for ITER FDR than for ITER FEAT, does not concord with the scientifically oriented question to reach $\{Q > 10\}$ to study the effects of predominant heating by alpha-particles, irrespective of the costs per (virtual) kwh. Therefore, we consider now the uncertainty propagation when keeping P_{aux} constant and changing P_{fus} and T so as to maximise Q.

— *4. Uncertainty propagation while maximising Q* —

This situation is rather complicated to analyse analytically. It is noted that Eq. (6) is an implicit equation for the operating temperature under stationary conditions ($d/dt(T) = 0$). The thermal (in-)stability of the operating point depends on the slope of the l.h.s. in Eq. 6 at the intersection point. If this slope exceeds 1, then not only the natural numerical iteration scheme to solve Eq. (6) diverges, but the operating point is also thermally unstable (in view of the time-derivative term in Eq. (6), so that active control is needed to keep the plasma at constant temperature.

On the other hand, when we consider the operating temperature as a free parameter, we can explicitly calculate P_{fus}, P_α and $P_{rad,\mathrm{ff}}$. If, in addition, we use an empirical scaling for the confinement time τ_E (replacing P_L by T), then we can also calculate explicitly, for each T, the amount of auxiliary heating power, P_{aux}, needed to sustain the temperature, and hence $Q = P_{fus}/P_{aux}$.

For practical evaluation we have written a direct integration routine in SAS [30], which determines, as a function of the central operating temperature T_c, the various contributions to the power balance using a flat density profile (with $n_e = 10^{20} m^{-3}$) and a simple class of temperature profiles:

$$
\begin{aligned}
T_e = & \\
& T_0(1 - x^4/w) \qquad \text{for} \quad 0 \le x \le c \qquad (\text{'sawtooth region'}) \\
& T_c(\frac{d-x}{d-c}) \qquad \text{for} \quad c \le x \le 1 \qquad (\text{'confinement region'})
\end{aligned}
$$

where $x = r/a$ is a normalised radial flux coordinate. The shapes of these profiles are in broad agreement with those in [31, 32]. The values of T_0 and w can be expressed in terms of T_c, c and d by the requirements that $T(x)$ and $d/dx T(x)$ are continuous at $x = c$. The reader is referred to Fig. 1 where, as in the subsequent results presented here, $c = 0.3$ and $d = 1.25$ has been used. (In Fig. 1, the profile has been normalised to $T_c = 1$.) For the total power balance, the precise radial dependence of $T(x)$ in the outer region of the plasma ($x > 0.8$) is not important.

For the radial integration also some information on how the flux-surface shape changes with radius is needed. From the information about equilibria available in the ITERH.DB3v5 database (excluding PBX-M), the following empirical expression for the contour length of the normalised flux-surface has been obtained:

$$L(x) = 2\pi(\kappa(x))^{1.0-0.85\ln\kappa(x)}(1 + \delta(x))^{0.12} x \qquad (11)$$

(The plasma cross-sectional area equals $a^2 \int_0^1 L(x)dx$. We approximate the volume by $2\pi R$ times the cross-sectional area.) From a few typical AUG equilibria, the crude approximation

$$\kappa(x) = 1.28(1 + 0.45x^3), \quad 1 + \delta(x) = 1 + 0.5x^3 \tag{12}$$

was used for an ITER reference plasma with $\kappa(1) = 1.86$ and $\delta(1) = 0.5$. This seems to be in reasonable agreement with [39] Fig. 3, however the central κ is somewhat higher in [40] Fig. 1. In Fig. 2, several heating powers and their ratios are displayed, on common logarithmic scale, as a function of the volume-average temperature $< T >$ (which for a flat n_e profile is proportional to the physically more meaningful quantity density-weighted volume-average temperature). Fig. 2^a displays the integrated heating power, P_α from the alpha particles according to Eqs. (6) and (7) and a temperature profile shape as specified above. Fig. 2^c gives the auxiliary power P_{aux} needed to reach the temperature $< T >$ under stationary conditions. The different curves correspond to different values of the proportionality factor H_H between the true confinement time in ITER FEAT and the point prediction from the ITERH-98P(y,2) scaling. In the region where the derivative of $\log P_{aux}$ with respect to $\log < T >$ is negative, the operating point is thermally unstable and active feedback control by P_{aux} (or possibly P_{rad}) is needed. We see that for $H_H = 1$, the equilibrium is stable for all temperatures. Fig. 2^b gives the power amplification factor $Q = P_{fus}/P_{aux}$ as a function of $< T >$ for several values of H_H. (Apart from a vertical shift this corresponds to the difference of the curves in Figs. 2^a and 2^c.) For $H_H > 1.25$ a temperature range exists where P_{aux} is zero and Q is infinitely large. For comparison, Fig. 2^d gives (again as a function of $< T >$ and for different values of H_H) the ratio $C = P_{fus}/P_L$, where P_L has been determined from ITERH-98P(y,2). From Fig. 2^d one can see, for instance, that for $H_H = 1$ the value $C = 6$ is reached at $\log < T >= 0.8$. It is noted that Fig. 2^b is a section from the POPCON plot (see [2] Ch.8, Fig.1) at constant density. The L-H and H-L transitions, which are not considered in this paper, lead to sudden changes in H_H. These occurs somewhere near the maxima of the curves in Fig. 2^b.

In Fig. 3^a we have plotted as a function of H_H (on the vertical axis) the maximum value of Q that can be reached by choosing a suitable operating temperature $< T >$, which has to be attained by adjusting P_{aux} as shown in Fig. 3^b. From Fig. 3^a one can see that an interval (0.8,1.2) for H_H translates into an interval $(5, \infty)$ for Q_{max}, whereas Fig. 3^b shows that about 45 MW auxiliary heating power is needed to achieve $Q_{max} = 5$ at $H_H = 0.8$.

Just for comparison, the parameters of the larger ITER FDR device, see [2], ($R = 8.14m$, $a = 2.8m$, $Vol = 2000m^3$, $I = 21MA$, $B_t = 5.68T$, $P_L \sim 200MW$, $P_{rad,xb}$ set to 60 MW), lead similarly to $Q_{max} = 10$ at $P_{aux} = 65MW$ for $H_H = 0.8$, provided ELMy H-mode is reached.

— *5. Fusion triple-product plot* —

Finally, one can represent the ignition curves from Fig. 2^b in an alternative way by plotting contours of constant Q in a plane described by the temperature along one axis and essentially the H_H factor along the other. As a variant of a familiar ignition-curve plot, we seek to plot $n^{\beta_n} T^{\beta_T} \tau_E$ against T, where β_n and β_T are chosen such that, according to a pertinent empirical confinement scaling, the quantity along the vertical axis is independent of T (and hence also of both P_L and P_{aux}) as well as independent of n. For ITERH-98P(y,2) with slightly rounded exponents, $\alpha_n = 0.4$ and $\alpha_P = 0.7$, we get $\beta_n = -(\alpha_n - \alpha_P)/(1 - \alpha_P) = 1$ and $\beta_T = \alpha_P/(1 - \alpha_P) = 7/3$. The practical results are shown in Fig. 4. (Note that now the 'central' temperature T_c instead of $< T >$ is plotted horizontally. This amounts to just an horizontal shift, since the profiles are assumed to be self-similar.) From Fig. 4 one can for instance see that the maximum attainable Q varies between 4 and ∞ when H_H varies between 0.7 and 1.4. It is noted that for an L-mode confinement scaling, such as ITER-89P, with $\alpha_n \simeq 0$ and $\alpha_P = 0.5$, we get, along the same line of argument, $\beta_n = 1$ and $\beta_T = 1$, which may in part explain the rationale for the traditional choice $nT\tau_E$ against T

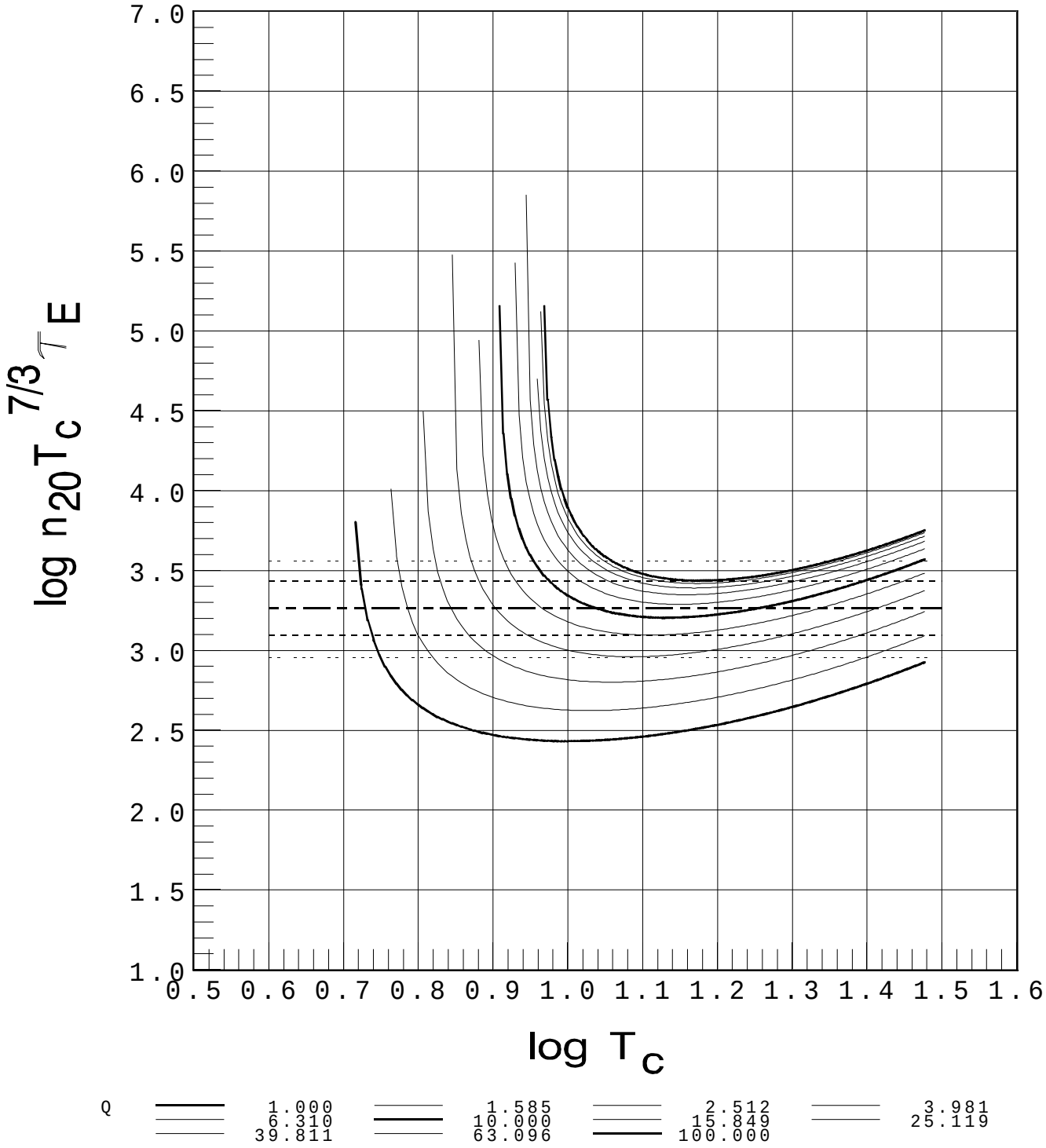

Figure 4: *The 'modified' fusion triple product $nT_c^{7/3}\tau_E$ against the 'central' temperature T_c, see Fig. 1. The vertical axis has been chosen such that for $\tau_{E,th} \simeq n^{0.4}P_L^{-0.7}$, as in ITERH-98P(y,2), the triple product is independent of n as well as of T_c (and hence of P_{aux}). The horizontal lines correspond to $H_H = 0.7, 0.82, 1.0, 1.22, 1.4$, respectively.*

when drawing ignition curves. The stronger power degradation in the more recently developed H and L-mode scalings suggests an improvement of this tradition.

— *Acknowledgements* —

The author gratefully acknowledges the initial inspiration from an E-mail discussion on this topic by several members of the ITER Joint Central Team (at Naka and Garching) during the last month of the previous century, provoked by the question from Prof. Dr. S.-I. Itoh and stimulated by Dr. V. Mukhovatov. He also much appreciated comments by Dr. Y. Murakami on the second draft of the manuscript as well as discussion in ITER JCT Physics Meetings and fruitful remarks by Dr. T. Takizuka. Prof. M. Bornatici, Dr. A. Costley and Prof. K. Lackner are acknowledged for drawing attention to some of the references. Part of this work was performed during a JAERI visiting scientist period in the Plasma Analysis Division of the Large Tokamak Facility at Naka Fusion Research Establishment, Japan.

References

[1] Feder, T., Physics Today, March 2000, 65.

[2] ITER Physics Basis Document, Nucl. Fusion **39** (1999), 2232.

[3] Kardaun, O., Plasma Phys. Control. Fusion **41** (1999), 429.

[4] Thomsen, K. for the H-mode Database Working Group, Nucl. Fusion **34** (1994) 131.

[5] Becker, G., Nucl. Fusion **39** (1999) 937.

[6] Rebhan E., Vieth, U., Reiter, D., Wolf, G.H., Nucl. Fusion **36** (1996) 264.

[7] Itoh, S.-I., ITER TAC Meeting, circulated letter (1999).

[8] Stotler, D.P., Goldston, R., Fusion Technology **20** (1991) 7.

[9] Kroese, A.H., Distributional inference: A loss function approach, Thesis Groningen, 1994.

[10] Zadeh, L.A., Kacprzyk, J., Fuzzy logic for the management of uncertainty, Academic Press, 1975.

[11] Shafer, G, A mathematical theory of evidence, Princeton University Press, 1976.

[12] Klir G.J., Yuan, B., Fuzzy sets and fuzzy logic, Prentice Hall, 1995

[13] Murakami, Y., et al. Probabilistic performance assessment of ITER FEAT, to be published.

[14] Mukhovatov, V., et al. Plasma Phys. Control. Fusion **42** (2000) A233.

[15] Zohm, H., Phys. Plasmas **4** (1997) 3433.

[16] Yu, Q., Günter, S., Giruzzi, G., Lackner, K., Zabiego, M., Physics of Plasmas **7** (2000) 312.

[17] Mitarai, O., Muraoka, K., Nucl. Fusion **39** (1999) 725.

[18] Bosch, H.-S., Hale, G.M., Nucl. Fusion **32** (1992) 611.

[19] Engelmann, F., Elementi di theoria della radiazione in un plasma, Laboratorio Gas Ionizzati 64/18 (1964).

[20] Borrass, K., Fusion Technology **16** (1989) 172.

[21] Bornatici, M., Cano, R., De Barbieri, O., Engelmann, F., Nucl. Fusion **23** (1983) 1153.

[22] Trubnikov, B.A., Bazhanova, A.E., in: Plasma Physics and the Problem of Controlled Nuclear Fusion (Ed. Leontovich, Tr. Sykes), Vol. III, Pergamon Press (1959) 141.

[23] Trubnikov, B.A., in: Вопросы Теории Плазмы, Атомиздат 1973. (Reviews of Plasma Physics **7** (1979) 345.)

[24] Campbell, D., Inversion of ECE emission from a tokamak plasma, PhD. Thesis (1981).

[25] Van Gelder, J.F.M., Westerhof, E., Schüller, F.C., Donné A.J.H., Plasma Phys. Control. Fusion **40** (1998) 1185.

[26] Hartfuß H.J., Geist, T., Hirsch M., Plasma Phys. Control. Fusion **39** (1997) 1693.

[27] Costley, A.E. and the TFR Group, Phys. Rev. Letters **38** (1977) 1477.

[28] Ségui, J.-L., et al., Nucl. Fusion **36** (1996) 237.

[29] Austin, M.E., Ellis, R.F., James, R.A., Luce, T.C. Phys. Plasmas **3** (1996) 3725.

[30] SAS Institute Inc., SAS/BASE Software, Release 6.12 (Cary NC).

[31] Becker, G., Nucl. Fusion **38** (1998) 293.

[32] Technical Basis for the ITER-FEAT Outline Design (2000), to be published.

[33] Ginzburg, V.L., Tsytovich, V. N., Transition radiation and transition scattering, Adam Hilger (1990), Bristol.

[34] Fidone, I., Meyer, R.L., Giruzzi, G., Granata, G., Phys. Fluids B **4** (1992) 4051.

[35] Romanelli, F., Giruzzi, G., Nucl. Fusion **38** (1998) 103.

[36] Fujita, T., et al., Nucl. Fusion **39** (1999) 1627.

[37] Neudatchin, S.V., et al., Plasma Phys. Control. Fusion **41** (1999) L39.

[38] Lang, P.T. et al., Nucl. Fusion **40** (2000) 245.

[39] Becker, G. in: European ITER Home Team: ITER Task S19 TP 05 FE (1998), NET report 111.

[40] Gribov, Y. et al., Task on ITER-FEAT PF Reference scenario: 15 MA plasma equilibrium snapshots (2000) ITER working memorandum.